scGRNom: a computational pipeline of integrative multi-omics analyses for predicting cell-type disease genes and regulatory networks

Ting Jin[1,2,*], Peter Rehani[2,3*], Mufang Ying[4,*], Jiawei Huang[4], Shuang Liu[2], Panagiotis Roussos[5,6], Daifeng Wang[1,2,7,#]

[1]Department of Biostatistics and Medical Informatics, University of Wisconsin – Madison, Madison, WI, 53706, USA

[2]Waisman Center, University of Wisconsin – Madison, Madison, WI, 53705, USA

[3]Department of Integrative Biology, University of Wisconsin - Madison, Madison, WI, 53706, USA

[4]Department of Statistics, University of Wisconsin - Madison, Madison, WI, 53706, USA

[5]Department of Psychiatry, Icahn School of Medicine at Mount Sinai, New York, NY, 10029, USA

[6]Department of Genetics and Genomic Sciences, Icahn School of Medicine at Mount Sinai, New York, NY, 10029, USA

[7]Department of Computer Sciences, University of Wisconsin – Madison, Madison, WI, 53706, USA

[*]equal contribution

[#]corresponding author

Short title: cell-type disease genes and networks from multi-omics

Keywords: Single-cell genomics; single-cell multi-omics integration; cell-type gene regulatory network; cell-type disease risk genes; cross-disease functional genomics; schizophrenia; Alzheimer's disease

Abstract

Understanding cell-type-specific gene regulatory mechanisms from genetic variants to diseases remains challenging. To address this, we developed an open-source computational pipeline, scGRNom, to predict the cell-type disease genes and regulatory networks from multi-omics data, including cell-type chromatin interactions, epigenomics, and single-cell transcriptomics. With applications to Schizophrenia and Alzheimer's Disease, our predicted cell-type regulatory networks link transcription factors and enhancers to disease genes for excitatory and inhibitory neurons, microglia, and oligodendrocytes. The enrichments of cell-type disease genes reveal cross-disease and disease-specific functions and pathways. Finally, machine learning analysis found that cell-type disease genes shared by diseases have improved clinical phenotype predictions.

Background

Recent Genome Wide Association Studies (GWAS) studies have identified a variety of genetic risk variants associated with multiple brain diseases. For example, a recent study found 109 pleiotropic loci significantly associated with at least two brain disorders [1]. Many cross-disease common genetic risk factors have revealed many shared functional consequences in clinical presentations [2]. Recent studies have also revealed shared symptoms at both psychiatric and physical levels between neurodegenerative and neuropsychiatric diseases [3]. For instance, 97% of Alzheimer's disease patients develop neuropsychiatric symptoms throughout the disease [4]. Besides, additional insights into each disease's progression and causes have further demonstrated the highly interlinked nature of both disease types [5]. However, our understanding of the molecular mechanisms of genetic variants between diseases remains elusive, particularly at the cell-type levels.

Alzheimer's disease (AD) and Schizophrenia (SCZ) are representative neurodegenerative and neuropsychiatric diseases, respectively. Both are significantly associated with genetic variants and have complex underlying cellular and molecular mechanisms from genotype to phenotype [6,7]. Notably, AD is physiologically characterized by accumulations of amyloid beta plaques and neurofibrillary tau protein tangles in the brain. Amyloid beta plaques primarily originate from the apolipoprotein E encoding gene APOE and its multiple variants. The APOE gene is a single step in the broader amyloidogenic processing pathway (APP), and additional genes involved in the process contribute to the regulation of amyloid beta production. Much work has identified major genes of interest involved in the APP. However, a distinct need still exists to further explore these disease loci to understand better the interplay between their regulatory elements and eventual amyloid beta creation and accumulation. Similarly, neurofibrillary tau tangles are associated with many genetic loci and require a study of the highly complex molecular mechanisms required to achieve disease pathology. Further, the downstream effects from both amyloid beta and neurofibrillary tangles within and between various cell types add additional complexity toward linking specific regulatory events and elements with clinical pathology [8,9].

Also, SCZ is a neuropsychiatric disorder characterized by disruptions in dopamine, glutamate, and GABA-based receptor signaling pathways. Pathologically, the direct connection is less clear between known molecular abnormalities and observed physical changes through neurological imaging studies. Thus, attempting to understand interactions between activation of known risk genes and higher-level pathway disruptions may help elucidate causes for structural shifts in SCZ patients. At a psychiatric level, the alterations to various cortical structures create multiple forms of symptoms, including positive (e.g., Hallucinogenic episodes) and negative (e.g., Anti-social tendencies). Finally, GWAS for AD cohorts has revealed multiple conserved genetic loci that could encode shared risk factors between the two diseases [10]. Clinical presentations, specifically psychiatric effects, create a crucial point of intersection to be explored where general psychosis was found in up to 60% of AD patients, including hallucination events as well as other effects mirroring those of the positive symptoms found in SCZ patients [11]. Thus, studying shared risk variants and genes between both diseases may help elucidate functional genomics of interest in both diseases. And it can further uncover cross-disease and disease-specific mechanisms between neurodegenerative and neuropsychiatric diseases.

Recently, advances in single-cell sequencing technologies have generated a great deal of excitement and interest in studying functional genomics at cellular resolution. For example, scRNA-seq and scATAC-seq techniques have measured the transcriptomics and epigenomics of individual cells in the human brain [12,13]. Further computational analyses have clustered cells into many cell types [12]. The cells in the same type share similar transcriptional activities such as gene expression and genomic functions. Differential gene expression across cell types is a complex, multi-gene dynamic process that tightly regulates and controls functions and is governed by gene regulatory factors such as transcriptional factors (TFs) and non-coding regulatory elements. These factors cooperate as a gene regulatory network (GRN) to facilitate the correct cellular and molecular functions on the genome-scale. Disrupted cooperation can give rise to abnormal gene expression, such as those present in diseases. Therefore, GRN has been used as robust system to infer genomic functions and molecular mechanisms, especially for human diseases [14].

Recent analyses have also revealed that brain disease risk variants are located in non-coding regulatory elements (e.g., enhancers). The risk genes likely have cell-type-specific effects for both neuronal and non-neuronal cell types [15,16]. Besides, recent single-cell studies suggest changes to cell-type-specific gene expression in brain diseases [8,9]. However, our understanding of the gene regulatory networks driving cell-type and disease-specific gene expression, especially across diseases, remains elusive. To address this issue, ones developed several computational methods to predict cell-type GRNs [17], such as PIDC [18], GENIE3 [19], and GRNBoost2 [20]. However, these methods typically only use single omics (e.g., transcriptomics) and predict networks based on statistical associations (e.g., co-expression), providing insufficient mechanistic insights into gene regulation at the cellular resolution. For instance, how the disease variants affect the transcription factor binding sites (TFBSs) on the distal regulatory elements (e.g., enhancers) that control disease genes is still unclear, especially at the cell-type level. Thus, it is essential to integrate emerging multi-omics data to understand cell-type gene regulation, especially involving non-coding regulatory elements. Recent studies have shown that integrating multi-omics data can reduce the impact of noise from a single omics data and achieve better prediction accuracy [21].

To explore these ideas, we developed a computational pipeline, scGRNom, by integrating multi-omics data to predict cell-type gene regulatory networks (GRNs) linking TFs, regulatory elements (e.g., enhancers and promoters), and target genes. In particular, we applied scGRNom to the multi-omics data at the cellular resolution, such as chromatin interactions, epigenomics, and single-cell transcriptomics of primary cell types in the human brain, including different excitatory and inhibitory neuronal types, microglia, and oligodendrocyte. Our predictions have high overlapping with state-of-the-art methods for revealing TFs and target genes [17], but they provide additional information on cell-type gene regulation, such as linking the regulatory elements to the genes. We also found that the enhancers in our cell-type GRNs are enriched with GWAS SNPs in human brain diseases, including psychiatric disorders and AD. Thus, we further linked the GWAS SNPs that interrupt TFBSs to cell-type disease genes based on the cell-type GRNs for SCZ and AD and found cross-disease and disease-specific genomic functions at the cell-type level. Finally, we found that the cell-type disease genes shared by AD and SCZ have improved predicting clinical phenotypes in AD, like disease staging and cognitive impairment.

Methods and Materials

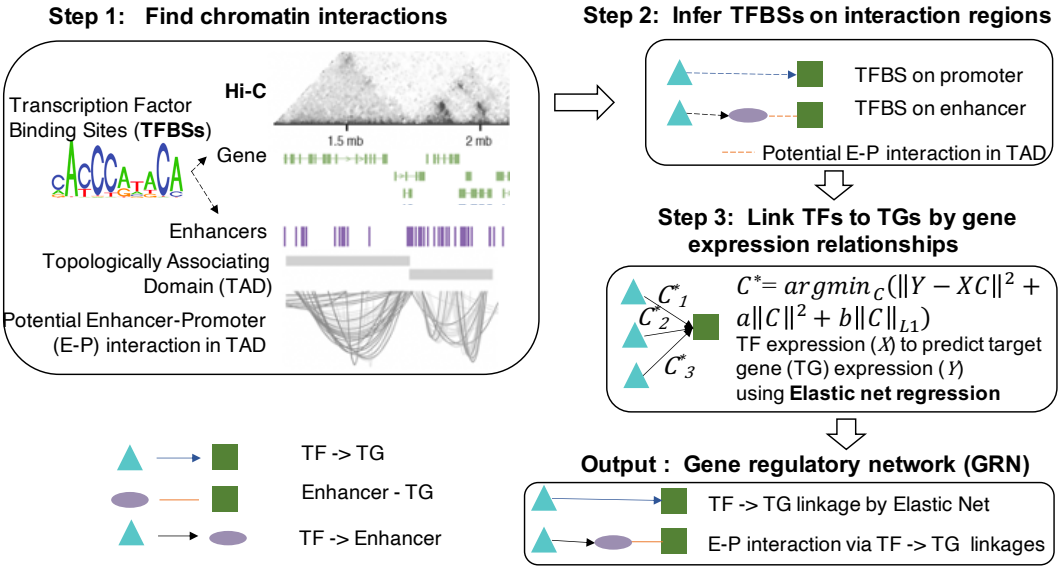

Figure 1. The computational pipeline, scGRNom, for predicting the gene regulatory network via multi-omics data. The pipeline inputs the chromatin interactions (e.g., from Hi-C) of regulatory elements (e.g., enhancer-promoter), identifies the transcription factor binding sites (TFBSs) on interacting regulatory elements, predicts TF-target gene expression relationships (e.g., high coefficients from Elastic net regression), and finally outputs a gene regulatory network linking TFs (cyan), regulatory elements (purple) to target genes (green).

Predicting gene regulatory networks from multi-omics data

scGRNom is a computational pipeline in R (https://github.com/daifengwanglab/scGRNom) to (I) integrate multi-omics datasets for predicting gene regulatory networks linking transcription factors, non-coding regulatory elements, and target genes, and (II) identify cell-type disease genes and regulatory elements. First, for predicting gene regulatory networks from multi-omics, scGRNom has three steps (**Figure 1**), each of which is available as an R function:

Step1: Finding chromatin interactions. The function, *scGRNom_interaction,* inputs the chromatin interaction data (e.g., Hi-C) and predicts all possible interactions between enhancers and promoters in the data or the user-provided list - for example, those from Topologically Associating Domains (TADs) in Hi-C data. In addition, the function uses an R package, *GenomicInteractions* [22], to annotate interacting regions and link them to genes;

Step 2: Inferring the transcription factor binding sites on interacting regions. The function, *scGRNom_getTF,* infers the transcription factor binding sites (TFBS) based on consensus binding site sequences in the enhancers and promoters that potentially interact from the previous step *scGRNom_interaction*. It outputs a reference gene regulatory network linking these TF, enhancers, and/or promoters of genes. In particular, this function uses *TFBSTools* [23] to obtain the position weight matrices of the TFBS motifs from the JASPAR database [24] and predicts the TFBS locations on the enhancers and promoters via mapping TF motifs. The function further links TFs with binding sites on all possible interacting enhancers and promoters and outputs the

reference regulatory network. Furthermore, this function can run on a parallel computing version via an R package, *motifmatchr* [25] for computational speed-up;

Step 3: Predicting the gene regulatory network. The function, *scGRNom_getNt* predicts the final gene regulatory network based on the TF-target gene expression relationships in the reference network. The reference gene regulatory network from the previous step provides all possible regulatory relationships (wires) between TF, enhancers, and target genes. However, the chromatin interacting regions are broad, so that many TFs likely have binding sites on them. Also, changes in gene expression may trigger different regulatory wires in the reference network. To refine our maps and determine the activity status of regulatory wires, we apply elastic net regression, a machine learning method that has successfully modeled TF-target gene expression relationships in the gene regulatory networks by our previous work [9]. Further, suppose the chromatin accessibility information is available (e.g., from scATAC-seq data for a cell type). In that case, the function can also filter the enhancers based on their chromatin accessibilities and then output the network links only having the enhancers with high accessibility (e.g., overlapped with scATAC-seq peaks). The parameter "open_chrom" inputs a list of user-defined chromatin accessible regions.

Mathematically, given a gene expression dataset and a reference network (e.g., from *scGRNom_getTF*), the function uses the TF expression to predict each target gene expression and finds the TF with high regression coefficients. Given a target gene, let $\boldsymbol{y} \in \mathcal{R}^n$ be a gene expression vector modeling its expression values across *n* samples (e.g., *n* cells from single cell data), and $\boldsymbol{X} \in \mathcal{R}^{n \times m}$ be the gene expression matrix of *m* TFs across *n* samples. Those *m* TFs should link to the target gene from the reference network, implying possible regulatory relationships to the gene. The elastic net regression model then aims to find the optimal coefficients for *m* TFs $\boldsymbol{c}^* \in \mathcal{R}^m$ to solve the following optimization problem:

$$\boldsymbol{c}^* = argmin_{\boldsymbol{c}}(\|\boldsymbol{y} - \boldsymbol{X}\boldsymbol{c}\|^2 + \alpha\|\boldsymbol{c}\|^2 + \beta\|\boldsymbol{c}\|_1),$$

where α and β are parameters to adjust the contributions from L_2 and L_1 regularizations of $\boldsymbol{c} \in \mathcal{R}^m$. The samples are randomly divided into the training and testing sets by the parameter, train_ratio (e.g., if train_ratio=0.7, then 70% training and 30% testing data). The optimal TF coefficients, $\boldsymbol{c}^*$ are estimated by the training data. Also, for the model evaluation, the mean square error (MSE) of the regression is calculated and reported by $\|\boldsymbol{y}_{\boldsymbol{test}} - \boldsymbol{X}_{\boldsymbol{test}}\boldsymbol{c}^*\|^2$ using the testing data. Further, the top TFs with high coefficients can be either selected by absolute coefficient values (the parameter, cutoff_absolute) or a percentage from all *m* TFs (the parameter, cutoff_percentage). Finally, the function outputs a final gene regulatory network linking the top TFs as well as their linked enhancers (from the reference network, if any) to all possible target genes.

Identifying cell-type disease genes and regulatory elements

In addition to predicting gene regulatory networks, the pipeline also provides another function, *scGRNom_disGenes,* for identifying cell-type disease genes and regulatory elements (e.g., enhancers, promoters). This function's input includes a cell-type gene regulatory network and a list of GWAS SNPs associated with a disease (**Figure 2**). The function uses an R package, *GenomicRanges* [26], to overlap these disease SNPs with the enhancers and promoters of the input cell-type gene regulatory network, and then find the ones that interrupt the binding sites of

all possible TFs (TFBSs) on the enhancers and promoters by *motifbreakR* [27]. It finally maps the overlapped enhancers or promoters and TFs with interrupted TFBSs onto the input network to find the linked genes and enhancers/promoters as the output cell-type disease genes and regulatory elements.

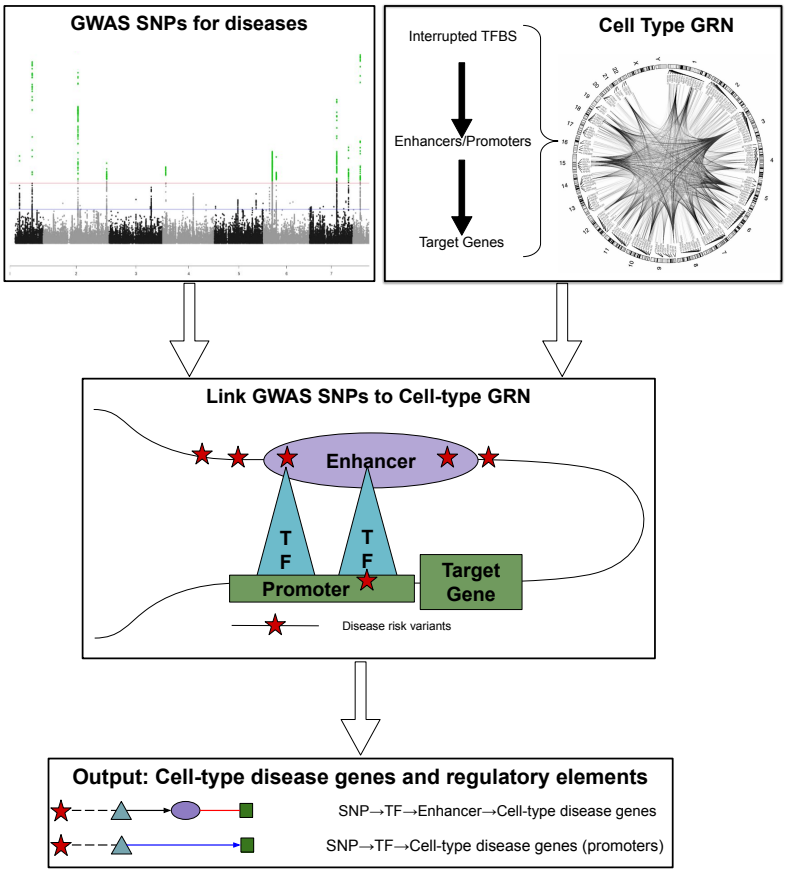

Figure 2. Identification of cell-type disease genes and regulatory elements. The function of our pipeline, *scGRNom_disGenes,* predicts cell-type disease genes and regulatory elements. First, it inputs a cell-type GRN (top right) and disease-associated SNPs from GWAS (top left). Second, the function identifies the disease SNPs that interrupt the binding sites of the TFs on the enhancers or promoters that link to the target genes in the input GRN (Middle). Finally, the function outputs a list of the target genes and regulatory elements (enhancers or promoters) linked by disease SNPs (Bottom). Red star: SNP. Cyan triangle: TF. Purple ellipse: Enhancer. Green square: cell-type disease gene.

Application to multi-omics data and data processing for predicting cell-type gene regulatory networks in the human brain

We applied our computational pipeline to the multi-omics datasets at the cellular resolution in the human brain. We predicted cell-type gene regulatory networks for major cell types: excitatory and inhibitory neurons, microglia, and oligodendrocyte for the human brain [12]. The excitatory neuronal types include Ex1, Ex2, Ex3e, Ex4, Ex5b, Ex6a, Ex6b, Ex8, and Ex9. The inhibitory neuronal types include In1a, In1b, In1c, In3, In4a, In4b, In6a, In6b, In7, and In8. We first input recently published cell-type chromatin interactome data in the human brain [15] to *scGRNom_interaction* to reveal all possible interactions from enhancers to gene promoters in the neuronal, microglia, and oligodendrocyte types. The genome annotation was from TxDb.Hsapiens.UCSC.hg19.knownGene [28]. We then predicted a reference regulatory network for each of these cell types using *scGRNom_getTF*. Finally, given a cell type, we input the single cell gene expression data for the type and the reference network from *scGRNom_getTF* to *scGRNom_getNt* for predicting the cell-type gene regulatory network (GRN).

Specifically, to make our predicted networks comparable across cell types, we made the following data preparation and processing steps. First, although different studies have generated increasing numbers of single cell data (e.g., for microglia [8]), we used the data from one study (GSE97942) [12] that includes the gene expression data (UMI) of individual cells of primary cell types, all from one postmortem tissue of human frontal cortex, aiming not to introduce additional batches from different studies, which helps our further comparative analyses across cell types. In addition, we filtered the genes that express in less than 100 cells. We then normalized gene expression by *Seurat 4.0* [29] for further removing noises and batches across cell types. We also applied the method *MAGIC* [30] to impute the single cell gene expression of all cells to address potential dropout issues. Then for each cell type, we removed the lowly expressed genes with log10(sum of imputed gene expression levels of the cells of the cell type+1) < 1. The numbers of genes and cells for each cell type used for prediction are available in Supplemental File 1.

For predicting a cell type GRN using the Elastic net regression model, we randomly split the cells into 70% training and 30% testing sets. We then selected the best Elastic net model that minimized the mean square error (MSE). We then filtered the target genes based on the goodness of fit by MSEs. In particular, we removed the target genes predicted by Elastic net regression with MSE > 0.1 and also TF-target gene with absolute Elastic net coefficient < 0.01. The output cell-type GRN consists of the network edges that link TFs, enhancers (if any), and target genes (TGs), as well as the Elastic net coefficient of TF-TGs for each edge. Finally, we provided two versions of each cell-type GRN (Supplemental File 2):

(I) the edges that include the enhancers that overlap the cell-type open chromatin regions predicted by recent scATAC-seq data (broad excitatory and inhibitory neurons, microglia and oligodendrocyte) [13];

(II) the edges that only include the top 10% TFs with absolute coefficients for each target gene without considering cell-type open chromatin regions (for scATAC-seq data might be likely noisy and no open chromatin regions available for neuronal subtypes).

Comparison with state-of-the-art methods

We compared our scGRNom predictions with existing state-of-the-art methods. In particular, we input the single-cell gene expression data for each cell type to a recently published benchmark framework, BEELINE [17], and predicted the cell-type regulatory networks using three of the most consistent and highly accurate methods, PIDC, GENIE3, and GRNBoost2. These methods only input gene expression data to predict all possible TF-target gene (TG) regulatory links based on their expression relationships, without considering the regulatory elements or open chromatin regions at the cell-type level. Thus, after applying to our processed single cell gene expression data, they generated more network edges than us because scGRNom only keeps the TF-TG links in which TFs have binding sites on the regulatory elements (e.g., enhancers and promoters). Therefore, to make these networks comparable with ours, we extended our networks by selecting up to the top 30% TFs for each TG and then checked if our TF-TG links predicted by the state-of-the-art method (also up to top 30% TFs for each TG selected for each method). In particular, given a cell-type GRN by scGRNom, we selected top K TFs per target gene (TG) to see if the TF-TG pairs were also predicted by PIDC, GENIE3, or GRNBoost2 (again picking top K TFs per TG). We varied K values from 0% to 30% and then calculated the percentages of the scGRNom's TF-TG pairs that can be predicted by one of those methods (Figure S1).

GWAS SNPs and heritability enrichment analyses for the enhancers in the cell-type gene regulatory networks in the human brain

Genome Wide Association Studies (GWAS) have identified a variety of genetic risk variants, including single nucleotide polymorphisms (SNPs) that are significantly associated with diseases and phenotypes (i.e., the traits). For example, recent GWAS studies have identified many SNPs associated with Alzheimer's Disease (AD, 2357 credible SNPs) [6] and Schizophrenia (SCZ, 6105 credible SNPs) [7]. In addition to the credible SNPs, we also included additional SNPs with p<5e-5 from the AD and SCZ GWAS summary statistics for linking potential additional cell-type disease genes [31]. We applied the *partitioned linkage disequilibrium score regression (LDSC)* [32] to evaluate the heritability explained by the enhancers of our cell-type gene regulatory networks for GWAS SNPs. In particular, our heritability enrichment analyses used the GWAS summary statistics for the diseases or traits: Schizophrenia (SCZ) [7], Alzheimer's disease (AD) [6], Autism spectrum disorder (ASD) [33], Bipolar disorder (BPD) [34], Amyotrophic lateral sclerosis (ALS) [35], Major depressive disorder (MDD) [36], Intelligence [37], Multiple sclerosis (MS) [38], Parkinson's disease (PD) [39], Attention deficit hyperactivity disorder (ADHD) [40], Education [41], Type 2 diabetes (T2D) [42], Inflammatory bowel disease (IBD) [43], Coronary artery disease (CAD) [44]. Also, we provided the numbers of GWAS SNPs for AD and SCZ that interrupt the binding sites of at least one of all possible TFBSs and the binding sites of the regulatory TFs in each cell-type GRN (Table S1).

Identification and enrichment analyses of cell-type disease genes

Given a cell-type and a disease type (AD or SCZ), we input the cell-type GRNs (both versions) and the GWAS SNPs for the disease to the *scGRNom_disGenes* function for identifying the cell-type disease genes. We identified the cell type disease genes (AD and SCZ) for all the cell types as above, including excitatory and inhibitory neuronal subtypes, microglia, and oligodendrocyte (Supplemental File 3). We also merged the disease genes for excitatory/inhibitory neuronal subtypes as the broad excitatory/inhibitory neuronal disease genes. We used the web app, *Metascape* [45] to find the enrichments of cell-type disease genes such as KEGG pathways, GO terms, protein-protein interactions, and diseases (via DisGeNET). Enrichment p-values shown in this paper were adjusted using the Benjamin-Hochberg (B-H) correction. Also, we looked at the expression levels of our cell-type disease genes in the disease samples. In particular, we compared the published population gene expression data in AD for single cell expression [8].

Machine learning prediction of clinical phenotypes from cell-type disease genes

Finally, we used the machine learning approach to predict clinical phenotypes from our cell-type disease genes using the population data of the ROSMAP project, an independent AD cohort [46]. Given a clinical phenotype, we assume that $X_i \in R^d$ represents the expression data of d disease genes for the ith individual in the cohort and $Y_i \in \{0,1\}$ represents the binarized class of the ith individual's phenotype with $i \in 1, \ldots, n$ individuals for training. We then found the optimal logistic regression model with the parameters $\{\beta_0^*, \beta_1^* \in R^d\}$ to classify the phenotype from the disease gene expression data via minimizing the following loss function:

$$\{\beta_0^*, \beta_1^*\} = argmax_{\beta_0,\beta_1} \sum_{i=1}^{n} -Y_i \log(\beta_0 + \beta_1^T X_i) - (1 - Y_i) \log(1 - \beta_0 - \beta_1^T X_i)$$

, where $(.)^T$ is the transpose operation. Also, we performed Cross-Validation (K=5) for the individual samples with 80% training and 20% testing sets. We also balanced the class sample size in each training set by the weighting method [47] so that the baseline of the classification accuracy is 50% for two classes. We used the individuals from the training sets to train the classification model. We then used the individuals from the testing sets to evaluate the classification performance, i.e., accuracy. In particular, we predicted four clinical phenotypes in ROSMAP: Braak Stages that measure the severity of neurofibrillary tangle (NFT) pathology (Braak early stages (0,1,2,3) vs. late stages (4, 5, 6)), CERAD scores that measure neuritic plaques (no AD vs. AD), the diagnosis of cognitive status (DCFDX, no or mild cognitive impairments (1,2,3) vs. Alzheimer's dementia (4, 5)) and the cognitive status at the time of death (COGDX, no or mild cognitive impairments (1,2,3) vs. Alzheimer's dementia (4, 5)).

Results

Predicting cell-type gene regulatory networks in the human brain

We applied the scGRNom pipeline to the multi-omics data for the human brain, including cell-type chromatin interactions [15], transcription factor binding sites [23], single-cell transcriptomics [9] and recent cell-type open chromatin regions [13] (Methods and Materials). In particular, we predicted the cell-type gene regulatory networks (GRNs) for both glial and neuronal types, including microglia, oligodendrocyte, excitatory neuronal subtypes (Ex1, Ex2, Ex3e, Ex4, Ex5b, Ex6a, Ex6b, Ex8 and Ex9, and inhibitory neuronal subtypes (In1a, In1b, In1c, In3, In4a, In4b, In6a, In6b, In7, and In8). Each cell-type GRN links TFs to enhancers to target genes (TGs), and has two versions that (I) only include the network edges with open cell-type enhancers predicted by recent scATAC-seq data [13] and (II) only include the edges with top 10% TFs with highest absolute coefficients for each target gene without using cell-type open chromatin regions (due to scATAC-seq data might be likely noisy and not specific to neuronal subtypes). For instance, we found that the microglia GRN with open chromatin regions consists of 47353 edges linking 180 TFs, 1893 microglia open enhancers, 1236 TGs. All cell-type GRNs are available in Supplemental File 2. The network statistics such as numbers of cells, edges, TFs, enhancers and TGs for all cell types are available in Supplemental File 1.

Our GRNs reveal many known cell-type-specific regulations. **Figure 3A** visualizes the subnetworks among TFs for select cell types (i.e., TGs are also TFs). For example, two known TFs, MEF2A and RFX3, that control microglia phenotypes play hub roles in the microglia network [48,49]. The nuclear factors NFIA, NFIX, and FOXP1 controlling neural differentiation and gliogenesis are also hub genes in the oligodendrocyte network [50–52]. MEF2C regulating inhibitory and excitatory synapses is a central node in both excitatory and inhibitory networks (e.g., Ex1 and In6b) [53]. In addition to cell-type TFs, we also observed the cell-type-specific expression relationships between TFs and TGs (high correlation). For instance, in **Figure 3B**, E2F3-LRRK2, STAT2-FBXO32, IRF2-DYNC1, and ATF4-EPB41L1 show cell-type-specific expression relationships across the cells of microglia, oligodendrocyte, Ex1, and In6b types.

337 In addition, we compared our predicted cell-type gene regulatory networks with existing state-of-
338 the-art methods for predicting cell-type gene regulatory networks, particularly those that are
339 consistent and highly accurate PIDC, GENIE3, and GRNBoost2 benchmarked by BEELINE [17]
340 (Materials and Methods). The percentages of the overlapped TF-TG links of the cell-type
341 network between scGRNom (both versions) and the state-of-the-art methods are over 50%
342 (Methods, **Figure S1**). This suggests a high consistency between scGRNom and these methods.
343 However, these methods predicted TF-TG links without providing information on regulatory
344 elements like enhancers. Thus, we looked further at the enhancers in our cell-type GRNs and
345 found that they have significantly high heritability enrichments for GWAS SNPs of multiple
346 brain diseases and traits ($p<0.05$, Materials and Methods). For example, the enhancers in our
347 excitatory-neuron and inhibitory-neuron GRNs have high enrichments for AD, SCZ, Major
348 depressive disorder, intelligence, education (**Figure 4A, Figure S2**). Besides, these brain-cell-
349 type enhancers do not have significant enrichment of GWAS SNPs for non-brain diseases.
350 Therefore, the heritability enrichment analysis suggests that the enhancers in our cell-type GRNs
351 have potential pleiotropic roles associated with multiple brain diseases or traits. Finally, we also
352 compared our cell-type networks with public GRN databases such as TRRUST [54], Dorothea
353 [55], and RegNetwork [56]. Those GRNs were primarily inferred by integrating different studies
354 from the literature (e.g., via physical interactions, co-expressed genes at the bulk tissue level) and
355 thus may not be specific for the neuronal and glial cell types in the human brain. However, we
356 still found many overlapped network edges (TF-TG) with our cell-type gene regulatory
357 networks. For example, we found that 319 TRRUST edges, 5935 Dorothea edges, 106
358 RegNetwork edges overlap with at least one of our cell-type GRNs, implying their potential
359 associations with the human brain's cell types.
360

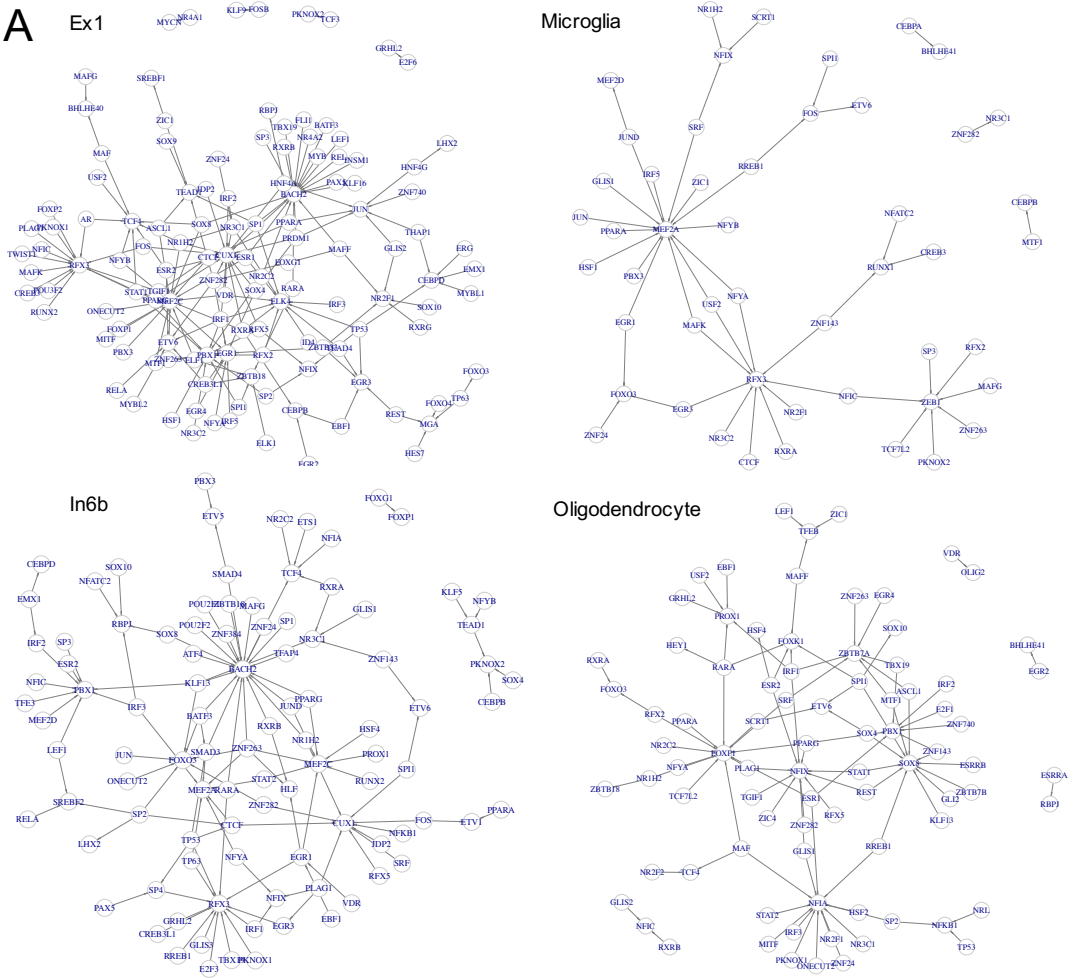
A
Ex1
Microglia
In6b
Oligodendrocyte

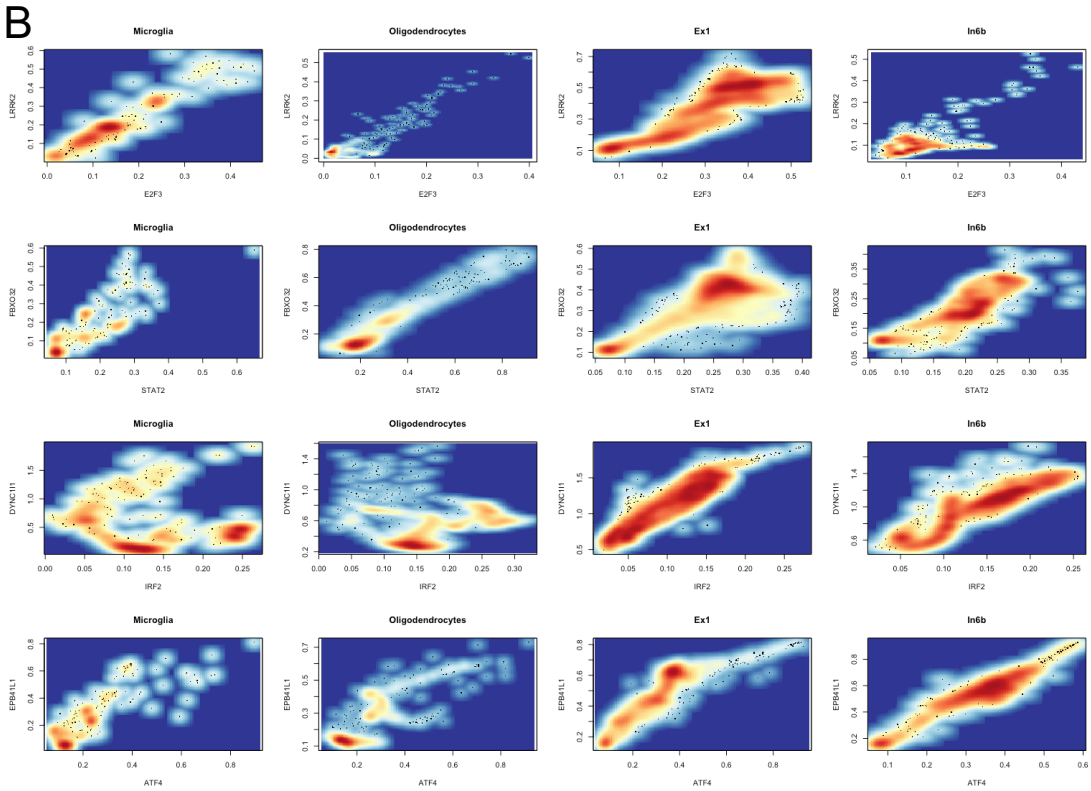
B
Microglia
Oligodendrocytes
Ex1
In6b
LRRK2
E2F3
FBXO32
STAT2
DYNC1I1
IRF2
EPB41L1
ATF4

Figure 3. Cell-type gene regulatory networks (GRNs) in the human brain. (**A**) The subnetworks of select cell-type GRNs among TFs (i.e., TG is also TF): Ex1 (Top left), Microglia (Top right), In6b (Bottom left), Oligodendrocyte (Bottom right). (**B**) The expression levels of the cells for select TFs and TGs across the four cell types in (**A**). TF: x-axis. TG: y-axis. The select TF-TG pairs from top to bottom are E2F3-LRRK2, STAT2-FBXO32, IRF2-DYNC1, and ATF4-EPB41L1. The red darkness corresponds to the expression level.

Identifying cell-type disease genes in AD and SCZ for neuronal and glial types

We used these cell-type GRNs to link GWAS SNPs with disease risk genes for each cell type, advancing knowledge on cross-disease and disease-specific interplays among genetic, transcriptional, and epigenetic risks at cellular resolution. In particular, we chose SCZ and AD, two majorly represented neuropsychiatric and neurodegenerative diseases with potential convergent underlying mechanisms [4], and we linked a number of cell-type disease genes (Methods, Supplemental File 3) and performed their enrichments (Supplemental File 4). We found that many disease genes present in one or a few cell types only, suggesting potential cell-type-specific contributions to AD and SCZ (**Figure S3**). As shown in **Figure 4B**, the cell-type AD genes are also significantly enriched with known disease genes for AD and other dementia diseases such as brain atrophy and cerebral amyloid angiopathy ($p<0.01$). For example, the microglia AD genes, including APP, CLU, BACE2, and BIN1, are specifically enriched for other diseases such as neurofibrillary degeneration, Parkinson's dementia, and aging memory impairment. Also, the cell-type SCZ genes are enriched for various disorders such as neurodevelopmental, mental and mood disorders, and depression ($p < 0.01$, **Figure 4C**). Furthermore, many cell-type disease genes have corresponding expression activities in the disease samples. For example, 72 excitatory AD genes (86%) and 65 inhibitory AD genes (80%) (plus 22 oligodendrocyte AD genes and three microglia AD genes) are significantly differentially expressed in the corresponding cell types in AD individuals, respectively ($p < 0.05$) [8].

The functional enrichment analyses for our cell-type disease genes also uncover known genomic functions and pathways at the cell-type level. For instance, the microglia AD genes are enriched with amyloid beta formation and clearance [57], MAPK signaling [58] and neuron death [59] (**Figure 4D**), and the oligodendrocyte AD genes are enriched with Tau protein binding [60]. This is vital to understanding a multitude of diseases that commonly demonstrate atrophy of cortical tissue as a hallmark feature. In SCZ genes, we also found that multiple key hallmark pathways were enriched, such as dopaminergic synapse [61], trans-synaptic signaling [62], and synapse organization [63] for excitatory SCZ genes (**Figure 4E**). For inhibitory SCZ genes, we observed that MAPK family signaling [64], regulation of NMDA receptor activity [65], dopaminergic synapses [61] and neurotransmission [65] are enriched.

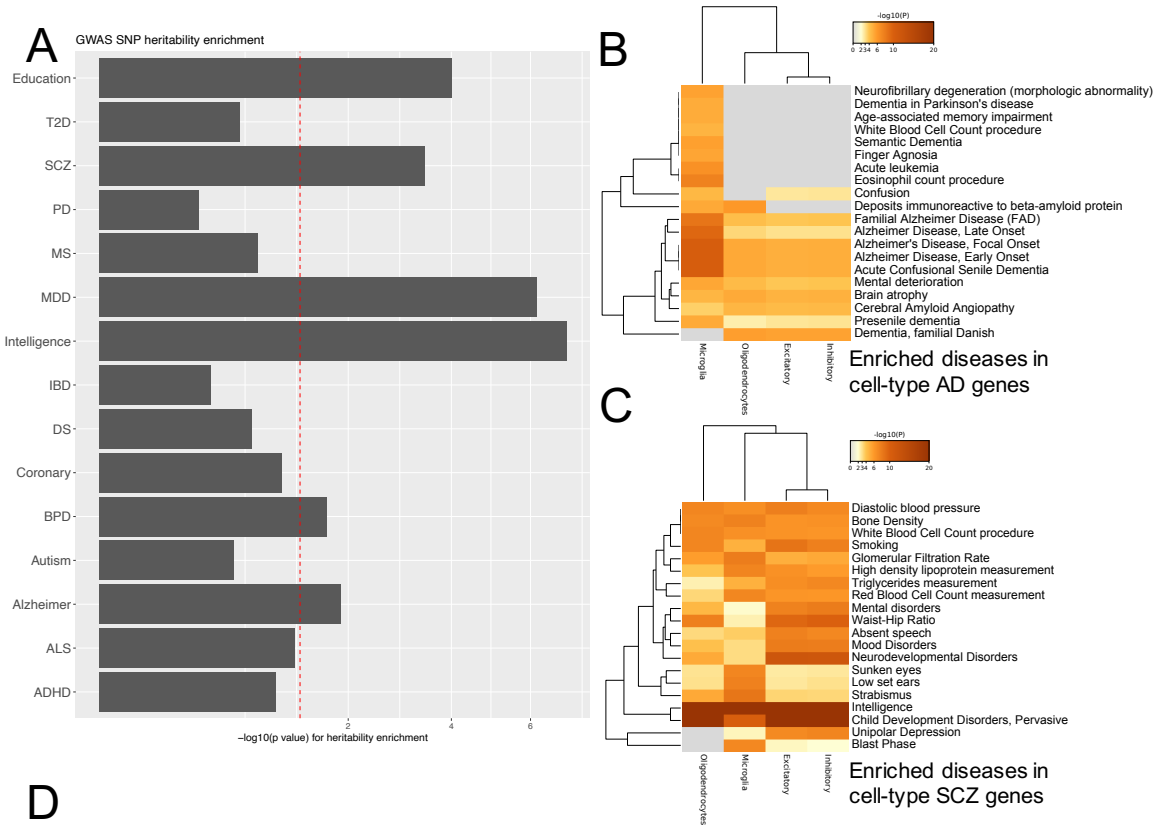
A
GWAS SNP heritability enrichment
Education
T2D
SCZ
PD
MS
MDD
Intelligence
IBD
DS
Coronary
BPD
Autism
Alzheimer
ALS
ADHD
–log10(p value) for heritability enrichment
B
-log10(P)
Neurofibrillary degeneration (morphologic abnormality)
Dementia in Parkinson's disease
Age-associated memory impairment
White Blood Cell Count procedure
Semantic Dementia
Finger Agnosia
Acute leukemia
Eosinophil count procedure
Confusion
Deposits immunoreactive to beta-amyloid protein
Familial Alzheimer Disease (FAD)
Alzheimer Disease, Late Onset
Alzheimer's Disease, Focal Onset
Alzheimer Disease, Early Onset
Acute Confusional Senile Dementia
Mental deterioration
Brain atrophy
Cerebral Amyloid Angiopathy
Presenile dementia
Dementia, familial Danish
Microglia
Oligodendrocytes
Excitatory
Inhibitory
Enriched diseases in cell-type AD genes
C
-log10(P)
Diastolic blood pressure
Bone Density
White Blood Cell Count procedure
Smoking
Glomerular Filtration Rate
High density lipoprotein measurement
Triglycerides measurement
Red Blood Cell Count measurement
Mental disorders
Waist-Hip Ratio
Absent speech
Mood Disorders
Neurodevelopmental Disorders
Sunken eyes
Low set ears
Strabismus
Intelligence
Child Development Disorders, Pervasive
Unipolar Depression
Blast Phase
Oligodendrocytes
Microglia
Excitatory
Inhibitory
Enriched diseases in cell-type SCZ genes

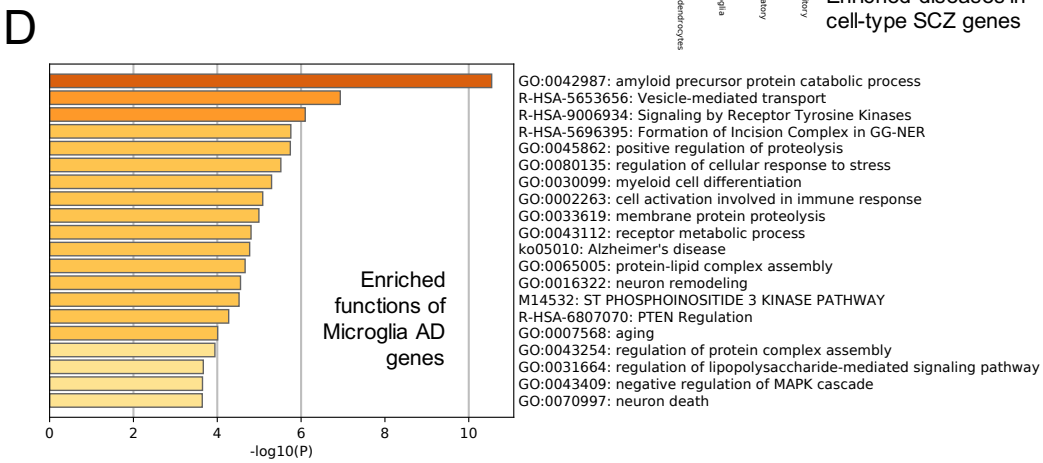
D
GO:0042987: amyloid precursor protein catabolic process
R-HSA-5653656: Vesicle-mediated transport
R-HSA-9006934: Signaling by Receptor Tyrosine Kinases
R-HSA-5696395: Formation of Incision Complex in GG-NER
GO:0045862: positive regulation of proteolysis
GO:0080135: regulation of cellular response to stress
GO:0030099: myeloid cell differentiation
GO:0002263: cell activation involved in immune response
GO:0033619: membrane protein proteolysis
GO:0043112: receptor metabolic process
ko05010: Alzheimer's disease
GO:0065005: protein-lipid complex assembly
GO:0016322: neuron remodeling
M14532: ST PHOSPHOINOSITIDE 3 KINASE PATHWAY
R-HSA-6807070: PTEN Regulation
GO:0007568: aging
GO:0043254: regulation of protein complex assembly
GO:0031664: regulation of lipopolysaccharide-mediated signaling pathway
GO:0043409: negative regulation of MAPK cascade
GO:0070997: neuron death
Enriched functions of Microglia AD genes
0
2
4
6
8
10
-log10(P)

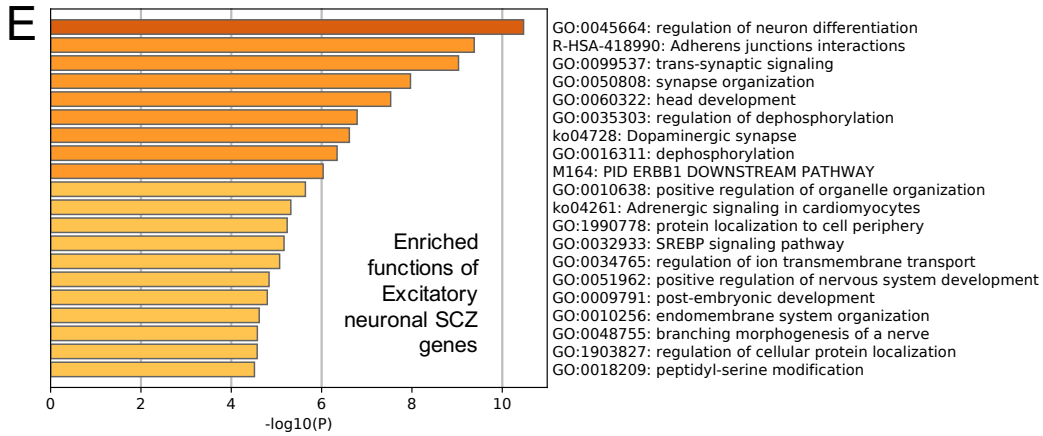
E
GO:0045664: regulation of neuron differentiation
R-HSA-418990: Adherens junctions interactions
GO:0099537: trans-synaptic signaling
GO:0050808: synapse organization
GO:0060322: head development
GO:0035303: regulation of dephosphorylation
ko04728: Dopaminergic synapse
GO:0016311: dephosphorylation
M164: PID ERBB1 DOWNSTREAM PATHWAY
GO:0010638: positive regulation of organelle organization
ko04261: Adrenergic signaling in cardiomyocytes
GO:1990778: protein localization to cell periphery
GO:0032933: SREBP signaling pathway
GO:0034765: regulation of ion transmembrane transport
GO:0051962: positive regulation of nervous system development
GO:0009791: post-embryonic development
GO:0010256: endomembrane system organization
GO:0048755: branching morphogenesis of a nerve
GO:1903827: regulation of cellular protein localization
GO:0018209: peptidyl-serine modification
Enriched functions of Excitatory neuronal SCZ genes
0
2
4
6
8
10
-log10(P)

Figure 4. Enrichments of cell-type enhancers and disease genes. (**A**) Partitioned heritability enrichment of GWAS SNPs associated with various diseases and traits (bar) on the enhancers of In1a GRN. Bar height is -log10(*p* value) of the enrichment. The diseases and traits are Schizophrenia (SCZ), Alzheimer's disease (AD), Autism spectrum disorder (ASD), Bipolar disorder (BPD), Amyotrophic lateral sclerosis (ALS), Major depressive disorder (MDD), Intelligence, Multiple sclerosis (MS), Parkinson's disease (PD), Attention deficit hyperactivity disorder (ADHD), Education, Type 2 diabetes (T2D), Inflammatory bowel disease (IBD), Coronary artery disease (CAD). The red line represents *p* value = 0.05. (**B**) The disease enrichments of cell-type AD genes. Rows are diseases/traits. Columns are cell types. Darkness is proportional to -log10(p) of the enriched term. (**C**) The disease enrichments of cell-type SCZ genes. Rows are diseases/traits. Columns are cell types. Darkness is proportional to -log10(p) of the enriched term. (**D**) The enrichments of functions and pathways (e.g., GO, KEGG, REACOME) in the microglia AD genes. Bar darkness and length are proportional to -log10(p) of the enriched term. (**E**) The enrichments of functions and pathways (e.g., GO, KEGG, REACOME) in the excitatory neuronal SCZ genes. Bar darkness and length are proportional to -log10(p) of the enriched term.

Comparative analyses reveal the interplays between genomic functions, pathways, cell types, and diseases

In addition to cell-type-specific pathways in these diseases, we also identified those involving multiple cell types in each disease, implying that potential cell-type interactions drive the disease pathology. For example, the enrichment of SCZ primarily includes changes in synapse structures and cell shaping and differentiation (**Figure 5A**). Clinically, this is consistent with the consensus that SCZ is strictly neuropsychiatric as opposed to degenerative. In particular, cell morphogenesis and regulation of neuron differentiation are enriched in all four major cell type SCZ genes ($p < 0.01$). Early life neurodevelopmental genetic markers may suggest causal links with alterations in hippocampal cell differentiation points on the front of cell morphogenesis, leading to cascades of downstream effects [66]. This has primarily been studied and modeled within the scope of iPSC-based analyses, which make correlations and connections to the clinical presentation more difficult due to the additional abstraction from the standard pathology-based analysis. Also, the BDNF signaling pathway that potentially relates to intercellular communications is enriched as well in multiple cell types ($p < 0.01$) [67]. Finally, we also observed that protein-protein interactions (PPIs) are enriched among the disease genes of the cell types at a higher level. As shown in **Figure 5B**, the SCZ genes for dopaminergic synapse, NMDA receptors, glutamate binding, and activation are shared by multiple cell types and have strong PPIs, implying protein-level cross-type coordination [68]. In AD, multiple pathways were significantly enriched across various cell types (**Figure 5C**). For instance, the catabolic process for the AD key player, amyloid precursor protein (APP) is enriched with both glial and neuronal types ($p < 0.01$) [69].

Furthermore, we found that cross-disease conserved functions/pathways are involved in one or multiple cell types, revealing potential novel functional interplays across cell types and diseases (**Figure 5D**). For example, the cell morphogenesis involved in differentiation is enriched in both AD and SCZ neuronal genes. Another example is that the vesicle-mediated transport is enriched for both AD and SCZ microglia genes. In total, we found 11 microglia genes shared by AD and SCZ. In particular, the VEGF signaling pathway is enriched in the SCZ microglia genes. In the general theme of AD pathology, increased VEGF expression has been linked to worse cognitive outcomes in post-mortem analysis [70]. Similarly, multiple meta analyses have revealed

differential expression levels between healthy controls and SCZ patients [71]. However, little has been done to link potential gene function to cell-type level interactions and pathways. Here, these SCZ-AD shared microglia genes may help explain shared higher-level dysfunction between both diseases as evidenced by higher expression. Also, we found that some functions involve different cell types across diseases. The dendrite development has been found in both SCZ and AD pathology [72,73]. We found that it is mainly enriched with microglia in AD but neuronal types in SCZ.

More interestingly, when exploring the interactions between cell types that change between diseases, the disease-specific pathologies enter to explain the cause of discrepancies. In particular, for AD, it is shown that phagocytic microglia are activated during the early stages of synaptic decline, leading to eventual neuroinflammation and programmed cell death [74]. For SCZ, the oligodendrocyte enrichment reveals similar intercellular mechanisms between excitatory and inhibitory neurons, specifically those regulating neuron differentiation (**Figure 5A**), providing potential direction for future exploration and validation of the communication role of oligodendrocytes [75].

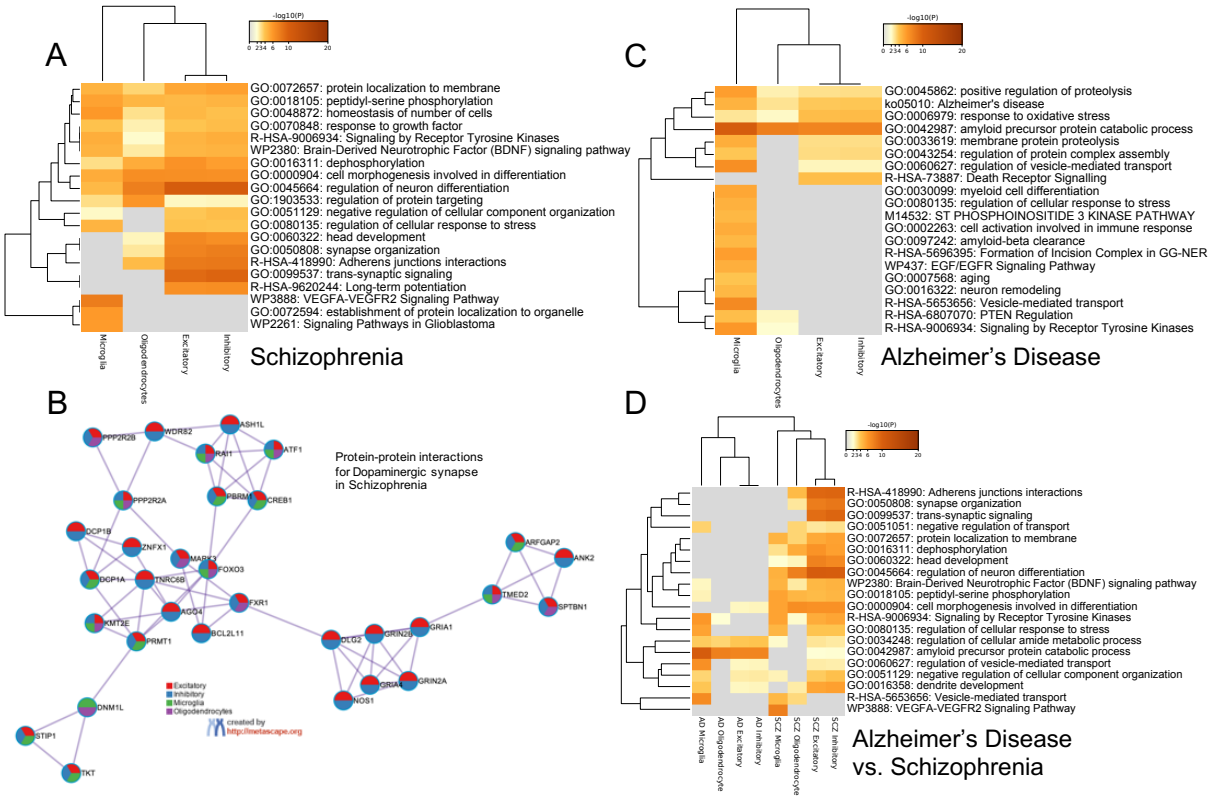

Figure 5. Cross-cell-type conserved and cell-type-specific functions, pathways and protein-protein interactions in Schizophrenia and Alzheimer's Disease. Darkness in heatmaps is proportional to -log10(p) of the enrichment. (**A**) The enrichments of select conserved and specific functions/pathways (e.g., GO, KEGG, REACTOME) across cell-type disease genes in Schizophrenia. (**B**) The enrichments of protein-protein interactions among major cell-type disease genes in Schizophrenia: Excitatory neuron (broad, red), Inhibitory neuron (broad, blue), Microglia (green), Oligodendrocyte (Purple). (**C**) The enrichments of select conserved and specific functions/pathways across cell-type disease genes in Alzheimer's Disease. (**D**) The enrichments of select conserved and specific functions/pathways across cell-type disease genes between Schizophrenia and Alzheimer's Disease.

Prediction of clinical phenotypes from cell-type disease genes

Finally, we want to investigate the clinical applications of our cell-type disease genes. To this end, we looked at the population-level gene expression data for Alzheimer's disease in the ROSMAP cohort [46]. In particular, we first found that many cell-type AD genes have significantly associated expression levels with clinical phenotypes across individuals in ROSMAP. For example, out of 195 cell-type AD genes, we found that 72 genes are significantly associated with the Braak Stages that measure the severity of neurofibrillary tangle (NFT) pathology (ANOVA $p < 0.05$), 78 genes with the CERAD scores that measure neuritic plaques (ANOVA $p < 0.05$), 89 genes with the diagnosis of cognitive status (DCFDX) (ANOVA $p < 0.05$), 73 genes with the cognitive status at the time of death (COGDX) (ANOVA $p < 0.05$) and 92 genes with the Mini-Mental State Examination (MMSE) scores (Pearson correlation $p < 0.05$). In total, 135 cell-type AD genes were significantly associated with at least one clinical phenotype in ROSMAP (Supplemental File 5).

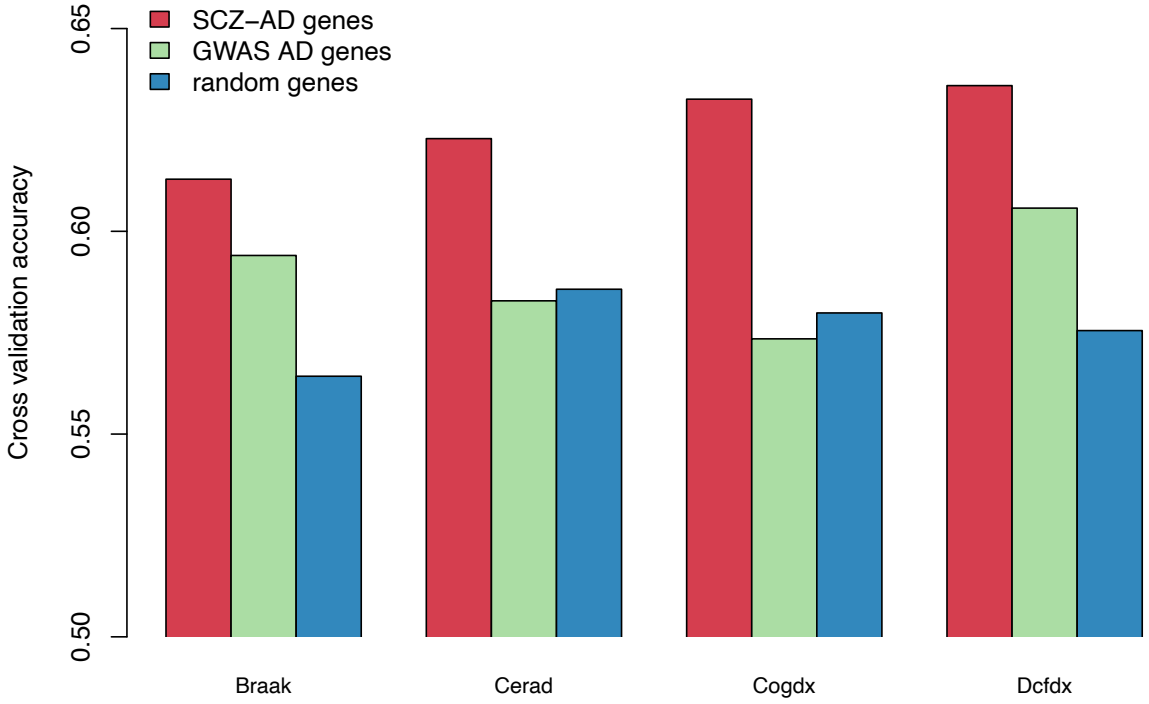

Figure 6. Prediction accuracy of AD clinical phenotypes from disease genes. The AD population data for prediction was from the ROSMAP cohort [46]. AD clinical phenotypes include Braak – stages that measure the severity of neurofibrillary tangle (NFT) pathology, Cerad – scores that measure neuritic plaques, Cogdx – cognitive status at the time of death, and Dcfdx - the diagnosis of cognitive status. The bar height represents the average accuracy of cross-validation (K=5) from the prediction using logistic regression (Methods). Red: scGRNom's cell-type disease genes shared by AD and SCZ (SCZ-AD genes). Green: AD genes from GWAS [6]. Blue: randomly select genes (same number as SCZ-AD genes).

In addition to statistically significant associations between our cell-type disease genes and clinical phenotypes, we also applied the machine learning approach to predict clinical phenotypes from these cell-type disease genes using ROSMAP data (Methods). Specifically, for each clinical phenotype, we used the logistic regression model to classify individual states of the phenotype (as classes) from their expression data of 53 AD-SCZ shared cell-type genes. We

performed the cross-validation (*K*=5) for the individual samples with 80% training and 20% testing sets. As shown in Fig. 6, our average accuracy values for classifying all four major clinical phenotypes: Braak Stages, CERAD scores, DCFDX status, COGDX status are much higher than the baselines (50%), the random select genes, and AD genes from the latest GWAS study [6]. This suggests that using cell-type disease genes shared by AD and SCZ has improved predicting those clinical phenotypes, especially for cognitive related ones in AD.

Discussion

This paper focuses on the scGRNom's application to single cell data for Alzheimer's and schizophrenia. However, scGRNom is general-purpose for understanding functional genomics and gene regulation in other diseases. Besides the cell types, the pipeline also predicts the gene regulatory networks for cell clusters (unknown cell types) and bulk tissue types. Furthermore, recent eQTL studies have identified various SNPs associating with gene expression in multiple brain tissue types using the population data such as GTEx [76] and PsychENCODE [9]. Although those brain eQTLs suggest the SNP-gene association at the bulk tissue level, we still found that several eQTLs in PsychENCODE match our linked GWAS SNPs and cell-type disease genes, e.g., SNPs chr2:127846321 for and chr20:43598154 for STK4, two microglia disease genes for AD and SCZ, respectively. This suggests potential cell-type effects of these human brain eQTLs. Thus, increasing single cell data at the population level allows us to predict the cell-type eQTLs [77], which will likely help understand cell-type gene regulation and refine linking disease genes at the cell-type level.

For linking disease genes, we primarily used the interrupted TFBSs by GWAS SNPs. Future studies utilizing scGRNom would be able to take advantage of the ever-growing number of GWAS for a wide variety of diseases as well as single cell data. However, additional information can also help link GWAS SNPs to disease genes. For example, existing tools such as FUMA [78] have linked GWAS loci to genes by integrating information from multiple resources, providing more functional linkages from genotype to genes to phenotype in human diseases. Thus, incorporating multiple GWAS data (e.g., various brain regions) exposes key areas of observed phenotypes. Previous studies have demonstrated the caution that must be exercised when attempting to correlate GWAS data with clinical phenotypes, and methods such as our analysis mitigate these effects [16]. A similar methodology as outlined could be used where common loci within each set of summary statistics are incorporated and established before integration into the cell type GRNs, thus linking neuronal spatial information with known mutation sites in patients along with potentially cell-type-specific functionality. Expanding past the cell types examined here into additional multicellular analyses is also possible given expanded interactome data. Notably, this would allow for further investigation of complex neuropsychological diseases and cases where the line between different clinical classifications becomes blurred and leads to additional complications about clinically relevant genetic therapies. One such example includes Autism Spectrum Disorder (ASD), where clinical presentations can vary in multiple axes of severity, creating a broad spectrum of phenotypes. In such cases, potentially linking specific symptoms or aspects of a particular subset of ASD to particular brain regions and cell types allows for a better-informed picture of functional consequences associated with genetic mutation sites. Such connections could aid in determining genetic risk factors associated with variations in edge case patients; they also create the opportunity to take advantage of Induced Pluripotent

Stem Cell (iPSC) technology using genetic engineering technologies to create point mutations matching computationally identified genes. Moreover, because the single cell multi-omics data we used for predicting cell-type GRNs are not specific for particular diseases (AD or SCZ), we used the SNPs disrupting all possible TFs on the enhancers and promoters from our cell type GRNs to link at large cell-type disease genes. However, the scGRNom pipeline is general-purpose and able to work for incoming disease-specific single cell multi-omics, and link to cell-type disease genes via interrupted regulatory TFs in the diseases.

Machine learning has also been widely used to analyze multi-omics, such as multiview learning and deep learning [9,79]. Multiview learning has great potential for understanding functional multi-omics and revealing nonlinear interactions across omics. Therefore, integrating such emerging machine learning approaches will enable identifying different cross-omic patterns, especially for increasing single-cell multi-omics data and providing more comprehensive mechanistic insights in cell-type gene regulation and linking to disease genes. For example, this means adding more omics such as methylation data that reflect epigenetic changes that may occur due to wide variations of inherited and environmental factors [80]. At a deeper functional level, variations in methylation have been attributed to alterations in splicing activity, ultimately impacting the regulation and expression of key genes [81]. Additionally, integrating proteomic data at a single-cell level enhances the broader picture formed through additional data sources even further [82]. Lastly, expanding past simple methylation and proteomics allows for the ability to include all forms of data incorporated through the single-cell cytometry [83].

Conclusions

We developed a computational pipeline, scGRNom, to integrate multi-omics data and predict gene regulatory networks (GRNs), which link TFs, non-coding regulatory elements (e.g., enhancers), and target genes. With applications to the data from single-cell multi-omics of the human brain, we predicted cell-type GRNs for both neuronal (e.g., excitatory, inhibitory) and glial cell types (e.g., microglia, oligodendrocyte). Further, scGRNom can input cell-type GRNs and disease risk variants to link disease genes at the cell-type level, such as brain diseases like Alzheimer's and schizophrenia. These disease genes revealed conserved and specific genomic functions across neuropsychiatric and neurodegenerative diseases, providing cross-disease regulatory mechanistic insights at the cellular resolution. Although this paper focuses on Alzheimer's and schizophrenia, scGRNom is general-purpose for understanding functional genomics and gene regulation in other diseases, at either bulk tissue or cell-type levels. Finally, scGRNom is open-source available at https://github.com/daifengwanglab/scGRNom.

Supplementary information

Supplemental materials – supplemental figures and table
Supplemental File 1 – statistics of cell-type gene regulatory networks
Supplemental File 2 – cell-type gene regulatory networks (TF, enhancer, target gene)
Supplemental File 3 – cell-type disease genes for AD and SCZ
Supplemental File 4 – enrichments of cell-type disease genes for AD and SCZ

548 Supplemental File 5 – cell-type disease genes associated with clinical phenotypes in AD

549 Data availability

550 Our pipeline for predicting gene regulatory networks via multi-omics is open-source available, as
551 well as a tutorial at https://github.com/daifengwanglab/scGRNom. All data supporting this study
552 are included in this paper, the supplemental files, and/or available from the corresponding author
553 on request.

554 Author contributions

555 D.W. conceived and designed the study. T.J. and M.Y. implemented the software. T.J., P.R.,
556 M.Y., J.H., S.L., and D.W. analyzed the data. T.J., P.R., M.Y. , Pa.R., and D.W wrote the
557 manuscript. All authors read and approved the final manuscript.

558 Competing interests

559 None declared.

560 Funding

561 This work was supported by the grants of National Institutes of Health, R01AG067025,
562 R21CA237955 and U01MH116492 to D.W., U54HD090256 to Waisman Center, and the start-
563 up funding for D.W. from the Office of the Vice Chancellor for Research and Graduate
564 Education at the University of Wisconsin–Madison.

565 References

566 1. Cross-Disorder Group of the Psychiatric Genomics Consortium. Electronic address:
567 plee0@mgh.harvard.edu, Cross-Disorder Group of the Psychiatric Genomics Consortium.
568 Genomic Relationships, Novel Loci, and Pleiotropic Mechanisms across Eight Psychiatric
569 Disorders. Cell. 2019;179:1469-1482.e11.

570 2. Brainstorm Consortium, Anttila V, Bulik-Sullivan B, Finucane HK, Walters RK, Bras J, et al.
571 Analysis of shared heritability in common disorders of the brain. Science. 2018;360.

572 3. Ciccocioppo F, Bologna G, Ercolino E, Pierdomenico L, Simeone P, Lanuti P, et al.
573 Neurodegenerative diseases as proteinopathies-driven immune disorders. Neural Regen Res.
574 2020;15:850–6.

575 4. Steinberg M, Shao H, Zandi P, Lyketsos CG, Welsh-Bohmer KA, Norton MC, et al. Point and 5-
576 year period prevalence of neuropsychiatric symptoms in dementia: the Cache County Study. Int
577 J Geriatr Psychiatry. 2008;23:170–7.

578 5. Cummings J, Ritter A, Rothenberg K. Advances in Management of Neuropsychiatric
579 Syndromes in Neurodegenerative Diseases. Curr Psychiatry Rep. 2019;21:79.

580 6. Jansen IE, Savage JE, Watanabe K, Bryois J, Williams DM, Steinberg S, et al. Genome-wide
581 meta-analysis identifies new loci and functional pathways influencing Alzheimer's disease risk.
582 Nat Genet. 2019;51:404–13.

583 7. Pardiñas AF, Holmans P, Pocklington AJ, Escott-Price V, Ripke S, Carrera N, et al. Common
584 schizophrenia alleles are enriched in mutation-intolerant genes and in regions under strong
585 background selection. Nat Genet. 2018;50:381–9.

586 8. Mathys H, Davila-Velderrain J, Peng Z, Gao F, Mohammadi S, Young JZ, et al. Single-cell
587 transcriptomic analysis of Alzheimer's disease. Nature. 2019;570:332–7.

588 9. Wang D, Liu S, Warrell J, Won H, Shi X, Navarro FCP, et al. Comprehensive functional genomic
589 resource and integrative model for the human brain. Science. 2018;362.

590 10. DeMichele-Sweet M a. A, Weamer EA, Klei L, Vrana DT, Hollingshead DJ, Seltman HJ, et al.
591 Genetic risk for schizophrenia and psychosis in Alzheimer disease. Mol Psychiatry. 2018;23:963–
592 72.

593 11. Murray PS, Kumar S, Demichele-Sweet MAA, Sweet RA. Psychosis in Alzheimer's disease.
594 Biol Psychiatry. 2014;75:542–52.

595 12. Lake BB, Chen S, Sos BC, Fan J, Kaeser GE, Yung YC, et al. Integrative single-cell analysis of
596 transcriptional and epigenetic states in the human adult brain. Nat Biotechnol. 2018;36:70–80.

597 13. Corces MR, Shcherbina A, Kundu S, Gloudemans MJ, Frésard L, Granja JM, et al. Single-cell
598 epigenomic analyses implicate candidate causal variants at inherited risk loci for Alzheimer's
599 and Parkinson's diseases. Nat Genet. 2020;52:1158–68.

600 14. Marbach D, Lamparter D, Quon G, Kellis M, Kutalik Z, Bergmann S. Tissue-specific regulatory
601 circuits reveal variable modular perturbations across complex diseases. Nat Methods.
602 2016;13:366–70.

603 15. Nott A, Holtman IR, Coufal NG, Schlachetzki JCM, Yu M, Hu R, et al. Brain cell type-specific
604 enhancer-promoter interactome maps and disease-risk association. Science. 2019;366:1134–9.

605 16. Sey NYA, Hu B, Mah W, Fauni H, McAfee JC, Rajarajan P, et al. A computational tool (H-
606 MAGMA) for improved prediction of brain-disorder risk genes by incorporating brain chromatin
607 interaction profiles. Nat Neurosci. 2020;

608 17. Pratapa A, Jalihal AP, Law JN, Bharadwaj A, Murali TM. Benchmarking algorithms for gene
609 regulatory network inference from single-cell transcriptomic data. Nat Methods. 2020;17:147–
610 54.

611 18. Chan TE, Stumpf MPH, Babtie AC. Gene Regulatory Network Inference from Single-Cell Data
612 Using Multivariate Information Measures. Cell Syst. 2017;5:251-267.e3.

613 19. Huynh-Thu VA, Irrthum A, Wehenkel L, Geurts P. Inferring regulatory networks from
614 expression data using tree-based methods. PloS One. 2010;5.

615 20. Moerman T, Aibar Santos S, Bravo González-Blas C, Simm J, Moreau Y, Aerts J, et al.
616 GRNBoost2 and Arboreto: efficient and scalable inference of gene regulatory networks.
617 Bioinforma Oxf Engl. 2019;35:2159–61.

618 21. Li Y, Wu F-X, Ngom A. A review on machine learning principles for multi-view biological data
619 integration. Brief Bioinform. 2018;19:325–40.

620 22. Harmston, N., Ing-Simmons, E., Perry, M., Baresic, A., Lenhard, B. GenomicInteractions: R
621 package for handling genomic interaction data [Internet]. 2020. Available from:
622 https://github.com/ComputationalRegulatoryGenomicsICL/GenomicInteractions/

623 23. Tan G, Lenhard B. TFBSTools: an R/bioconductor package for transcription factor binding
624 site analysis. Bioinforma Oxf Engl. 2016;32:1555–6.

625 24. Fornes O, Castro-Mondragon JA, Khan A, van der Lee R, Zhang X, Richmond PA, et al.
626 JASPAR 2020: update of the open-access database of transcription factor binding profiles.
627 Nucleic Acids Res. 2020;48:D87–92.

628 25. Schep, Alicia. motifmatchr: Fast Motif Matching in R [Internet]. 2019. Available from:
629 https://www.bioconductor.org/packages/release/bioc/html/motifmatchr.html

630 26. Lawrence M, Huber W, Pagès H, Aboyoun P, Carlson M, Gentleman R, et al. Software for
631 computing and annotating genomic ranges. PLoS Comput Biol. 2013;9:e1003118.

632 27. Coetzee SG, Coetzee GA, Hazelett DJ. motifbreakR: an R/Bioconductor package for
633 predicting variant effects at transcription factor binding sites. Bioinforma Oxf Engl.
634 2015;31:3847–9.

635 28. Carlson, Marc. TxDb.Hsapiens.UCSC.hg19.knownGene: Annotation package for TxDb
636 object(s) [Internet]. Bioconductor; 2015. Available from:
637 https://bioconductor.org/packages/release/data/annotation/html/TxDb.Hsapiens.UCSC.hg19.k
638 nownGene.html

639 29. Stuart T, Butler A, Hoffman P, Hafemeister C, Papalexi E, Mauck WM, et al. Comprehensive
640 Integration of Single-Cell Data. Cell. 2019;177:1888-1902.e21.

641 30. van Dijk D, Sharma R, Nainys J, Yim K, Kathail P, Carr AJ, et al. Recovering Gene Interactions
642 from Single-Cell Data Using Data Diffusion. Cell. 2018;174:716-729.e27.

643 31. Panagiotou OA, Ioannidis JPA, for the Genome-Wide Significance Project. What should the
644 genome-wide significance threshold be? Empirical replication of borderline genetic
645 associations. Int J Epidemiol. 2012;41:273–86.

646 32. Finucane HK, Bulik-Sullivan B, Gusev A, Trynka G, Reshef Y, Loh P-R, et al. Partitioning
647 heritability by functional annotation using genome-wide association summary statistics. Nat
648 Genet. 2015;47:1228–35.

649 33. Cross-Disorder Group of the Psychiatric Genomics Consortium. Identification of risk loci with
650 shared effects on five major psychiatric disorders: a genome-wide analysis. Lancet Lond Engl.
651 2013;381:1371–9.

652 34. Psychiatric GWAS Consortium Bipolar Disorder Working Group. Large-scale genome-wide
653 association analysis of bipolar disorder identifies a new susceptibility locus near ODZ4. Nat
654 Genet. 2011;43:977–83.

655 35. van Rheenen W, Shatunov A, Dekker AM, McLaughlin RL, Diekstra FP, Pulit SL, et al.
656 Genome-wide association analyses identify new risk variants and the genetic architecture of
657 amyotrophic lateral sclerosis. Nat Genet. 2016;48:1043–8.

658 36. Howard DM, Adams MJ, Clarke T-K, Hafferty JD, Gibson J, Shirali M, et al. Genome-wide
659 meta-analysis of depression identifies 102 independent variants and highlights the importance
660 of the prefrontal brain regions. Nat Neurosci. 2019;22:343–52.

661 37. Savage JE, Jansen PR, Stringer S, Watanabe K, Bryois J, de Leeuw CA, et al. Genome-wide
662 association meta-analysis in 269,867 individuals identifies new genetic and functional links to
663 intelligence. Nat Genet. 2018;50:912–9.

664 38. International Multiple Sclerosis Genetics Consortium, Wellcome Trust Case Control
665 Consortium 2, Sawcer S, Hellenthal G, Pirinen M, Spencer CCA, et al. Genetic risk and a primary
666 role for cell-mediated immune mechanisms in multiple sclerosis. Nature. 2011;476:214–9.

667 39. Blauwendraat C, Heilbron K, Vallerga CL, Bandres-Ciga S, von Coelln R, Pihlstrøm L, et al.
668 Parkinson's disease age at onset genome-wide association study: Defining heritability, genetic
669 loci, and α-synuclein mechanisms. Mov Disord Off J Mov Disord Soc. 2019;34:866–75.

670 40. Demontis D, Walters RK, Martin J, Mattheisen M, Als TD, Agerbo E, et al. Discovery of the
671 first genome-wide significant risk loci for attention deficit/hyperactivity disorder. Nat Genet.
672 2019;51:63–75.

673 41. Okbay A, Beauchamp JP, Fontana MA, Lee JJ, Pers TH, Rietveld CA, et al. Genome-wide
674 association study identifies 74 loci associated with educational attainment. Nature.
675 2016;533:539–42.

676 42. Morris AP, Voight BF, Teslovich TM, Ferreira T, Segrè AV, Steinthorsdottir V, et al. Large-
677 scale association analysis provides insights into the genetic architecture and pathophysiology of
678 type 2 diabetes. Nat Genet. 2012;44:981–90.

679 43. Jostins L, Ripke S, Weersma RK, Duerr RH, McGovern DP, Hui KY, et al. Host-microbe
680 interactions have shaped the genetic architecture of inflammatory bowel disease. Nature.
681 2012;491:119–24.

682 44. Schunkert H, König IR, Kathiresan S, Reilly MP, Assimes TL, Holm H, et al. Large-scale
683 association analysis identifies 13 new susceptibility loci for coronary artery disease. Nat Genet.
684 2011;43:333–8.

685 45. Zhou Y, Zhou B, Pache L, Chang M, Khodabakhshi AH, Tanaseichuk O, et al. Metascape
686 provides a biologist-oriented resource for the analysis of systems-level datasets. Nat Commun.
687 2019;10:1523.

688 46. De Jager PL, Ma Y, McCabe C, Xu J, Vardarajan BN, Felsky D, et al. A multi-omic atlas of the
689 human frontal cortex for aging and Alzheimer's disease research. Sci Data. 2018;5:180142.

690 47. King G, Zeng L. Logistic Regression in Rare Events Data. Polit Anal. 2001;9:137–63.

691 48. Holtman IR, Skola D, Glass CK. Transcriptional control of microglia phenotypes in health and
692 disease. J Clin Invest. 2017;127:3220–9.

693 49. Zeisel A, Munoz-Manchado AB, Codeluppi S, Lonnerberg P, La Manno G, Jureus A, et al. Cell
694 types in the mouse cortex and hippocampus revealed by single-cell RNA-seq. Science.
695 2015;347:1138–42.

696 50. Deneen B, Ho R, Lukaszewicz A, Hochstim CJ, Gronostajski RM, Anderson DJ. The
697 Transcription Factor NFIA Controls the Onset of Gliogenesis in the Developing Spinal Cord.
698 Neuron. 2006;52:953–68.

699 51. Zhou B, Osinski JM, Mateo JL, Martynoga B, Sim FJ, Campbell CE, et al. Loss of NFIX
700 Transcription Factor Biases Postnatal Neural Stem/Progenitor Cells Toward Oligodendrogenesis.
701 Stem Cells Dev. 2015;24:2114–26.

702 52. Pearson CA, Moore DM, Tucker HO, Dekker JD, Hu H, Miquelajáuregui A, et al. Foxp1
703 Regulates Neural Stem Cell Self-Renewal and Bias Toward Deep Layer Cortical Fates. Cell Rep.
704 2020;30:1964-1981.e3.

705 53. Harrington AJ, Raissi A, Rajkovich K, Berto S, Kumar J, Molinaro G, et al. MEF2C regulates
706 cortical inhibitory and excitatory synapses and behaviors relevant to neurodevelopmental
707 disorders. eLife. 2016;5.

708 54. Han H, Cho J-W, Lee S, Yun A, Kim H, Bae D, et al. TRRUST v2: an expanded reference
709 database of human and mouse transcriptional regulatory interactions. Nucleic Acids Res.
710 2018;46:D380–6.

711 55. Garcia-Alonso L, Holland CH, Ibrahim MM, Turei D, Saez-Rodriguez J. Benchmark and
712 integration of resources for the estimation of human transcription factor activities. Genome
713 Res. 2019;29:1363–75.

714 56. Liu Z-P, Wu C, Miao H, Wu H. RegNetwork: an integrated database of transcriptional and
715 post-transcriptional regulatory networks in human and mouse. Database. 2015;2015:bav095.

716 57. Baik SH, Kang S, Son SM, Mook-Jung I. Microglia contributes to plaque growth by cell death
717 due to uptake of amyloid β in the brain of Alzheimer's disease mouse model. Glia.
718 2016;64:2274–90.

719 58. Kheiri G, Dolatshahi M, Rahmani F, Rezaei N. Role of p38/MAPKs in Alzheimer's disease:
720 implications for amyloid beta toxicity targeted therapy. Rev Neurosci. 2018;30:9–30.

721 59. Marín-Teva JL, Cuadros MA, Martín-Oliva D, Navascués J. Microglia and neuronal cell death.
722 Neuron Glia Biol. 2011;7:25–40.

723 60. Barbier P, Zejneli O, Martinho M, Lasorsa A, Belle V, Smet-Nocca C, et al. Role of Tau as a
724 Microtubule-Associated Protein: Structural and Functional Aspects. Front Aging Neurosci.
725 2019;11:204.

726 61. McCutcheon RA, Krystal JH, Howes OD. Dopamine and glutamate in schizophrenia: biology,
727 symptoms and treatment. World Psychiatry Off J World Psychiatr Assoc WPA. 2020;19:15–33.

728 62. Berdenis van Berlekom A, Muflihah CH, Snijders GJLJ, MacGillavry HD, Middeldorp J, Hol
729 EM, et al. Synapse Pathology in Schizophrenia: A Meta-analysis of Postsynaptic Elements in
730 Postmortem Brain Studies. Schizophr Bull. 2020;46:374–86.

731 63. Osimo EF, Beck K, Reis Marques T, Howes OD. Synaptic loss in schizophrenia: a meta-
732 analysis and systematic review of synaptic protein and mRNA measures. Mol Psychiatry.
733 2019;24:549–61.

734 64. McGuire JL, Depasquale EA, Funk AJ, O'Donnovan SM, Hasselfeld K, Marwaha S, et al.
735 Abnormalities of signal transduction networks in chronic schizophrenia. NPJ Schizophr.
736 2017;3:30.

737 65. Kehrer C, Maziashvili N, Dugladze T, Gloveli T. Altered Excitatory-Inhibitory Balance in the
738 NMDA-Hypofunction Model of Schizophrenia. Front Mol Neurosci. 2008;1:6.

739 66. Ahmad R, Sportelli V, Ziller M, Spengler D, Hoffmann A. Tracing Early Neurodevelopment in
740 Schizophrenia with Induced Pluripotent Stem Cells. Cells. 2018;7.

741 67. Sasi M, Vignoli B, Canossa M, Blum R. Neurobiology of local and intercellular BDNF signaling.
742 Pflüg Arch - Eur J Physiol. 2017;469:593–610.

743 68. Fabiani C, Antollini SS. Alzheimer's Disease as a Membrane Disorder: Spatial Cross-Talk
744 Among Beta-Amyloid Peptides, Nicotinic Acetylcholine Receptors and Lipid Rafts. Front Cell
745 Neurosci. 2019;13:309.

746 69. O'Brien RJ, Wong PC. Amyloid precursor protein processing and Alzheimer's disease. Annu
747 Rev Neurosci. 2011;34:185–204.

748 70. Mahoney ER, Dumitrescu L, Moore AM, Cambronero FE, De Jager PL, Koran MEI, et al. Brain
749 expression of the vascular endothelial growth factor gene family in cognitive aging and
750 alzheimer's disease. Mol Psychiatry. 2019;

751 71. Misiak B, Stramecki F, Stańczykiewicz B, Frydecka D, Lubeiro A. Vascular endothelial growth
752 factor in patients with schizophrenia: A systematic review and meta-analysis. Prog
753 Neuropsychopharmacol Biol Psychiatry. 2018;86:24–9.

754 72. Glausier JR, Lewis DA. Dendritic spine pathology in schizophrenia. Neuroscience.
755 2013;251:90–107.

756 73. Cochran JN, Hall AM, Roberson ED. The dendritic hypothesis for Alzheimer's disease
757 pathophysiology. Brain Res Bull. 2014;103:18–28.

758 74. Fakhoury M. Microglia and Astrocytes in Alzheimer's Disease: Implications for Therapy. Curr
759 Neuropharmacol. 2018;16:508–18.

760 75. Raabe FJ, Slapakova L, Rossner MJ, Cantuti-Castelvetri L, Simons M, Falkai PG, et al.
761 Oligodendrocytes as A New Therapeutic Target in Schizophrenia: From Histopathological
762 Findings to Neuron-Oligodendrocyte Interaction. Cells. 2019;8.

763 76. GTEx Consortium. The Genotype-Tissue Expression (GTEx) project. Nat Genet. 2013;45:580–
764 5.

765 77. Kim-Hellmuth S, Aguet F, Oliva M, Muñoz-Aguirre M, Kasela S, Wucher V, et al. Cell type–
766 specific genetic regulation of gene expression across human tissues. Science.
767 2020;369:eaaz8528.

768 78. Watanabe K, Taskesen E, van Bochoven A, Posthuma D. Functional mapping and annotation
769 of genetic associations with FUMA. Nat Commun. 2017;8:1826.

770 79. Nguyen ND, Wang D. Multiview learning for understanding functional multiomics. PLoS
771 Comput Biol. United States; 2020;16:e1007677.

772 80. Lacal I, Ventura R. Epigenetic Inheritance: Concepts, Mechanisms and Perspectives. Front
773 Mol Neurosci. 2018;11:292.

774 81. Linker SM, Urban L, Clark SJ, Chhatriwala M, Amatya S, McCarthy DJ, et al. Combined single-
775 cell profiling of expression and DNA methylation reveals splicing regulation and heterogeneity.
776 Genome Biol. 2019;20:30.

777 82. Marx V. A dream of single-cell proteomics. Nat Methods. 2019;16:809–12.

778 83. Brummelman J, Haftmann C, Núñez NG, Alvisi G, Mazza EMC, Becher B, et al. Development,
779 application and computational analysis of high-dimensional fluorescent antibody panels for
780 single-cell flow cytometry. Nat Protoc. 2019;14:1946–69.

781